ECCOMAS Congress 2016
VII European Congress on Computational Methods in Applied Sciences and Engineering
M. Papadrakakis, V. Papadopoulos, G. Stefanou, V. Plevris (eds.)
Crete Island, Greece, 5–10 June 2016

A 3D ELECTROMECHANICAL FEM-BASED MODEL FOR CARDIAC TISSUE

Minh Tuan Duong[1,2], **Alexander Jung**[1], **Ralf Frotscher**[1] **and Manfred Staat**[1]

[1] Aachen University of Applied Sciences
Institute of Bioengineering
Heinrich-Mußmann-Str. 1, 52428 Jülich, Germany
e-mail: {a.jung, frotscher, m.staat}@fh-aachen.de

[2] Hanoi University of Science and Technology
DaiCoViet No.1, Hanoi, Vietnam
tuan.duongminh@hust.edu.vn

Keywords: Cardiac Tissue, CellDrum, Cell Models, Drug Modeling, Electromechanical Coupling

Abstract. *The CellDrum provides an experimental setup to investigate the electromechanics of a cardiac tissue construct and particularly the effect of drugs. Experimental data can be used to parametrize and validate computational electromechanical models. Until now, the experiments have been performed with a thin tissue layer of a mixture including ventricular, atrial and sinoatrial cells. Mechanically, it is modeled as a materially and geometrically nonlinear shell. For future experiments with a thick tissue layer of mixtures and single cardiac cell types the mechanical model is extended to a nonlinear 3D continuum which can be used as a step towards whole heart modeling. Comparisons with the 2D shell model are presented with and without the consideration of a chosen drug and a simulation with a model for thick cardiac tissue construct is carried out to give a first impression on how the experiments might look like.*

1 INTRODUCTION

A human heart is divided into four chambers, two atria and two ventricles, connected by four valves. The right atrium receives oxygen-poor blood from the body and pumps it to the right ventricle from where it is pumped to the lungs. The left atrium receives oxygen-rich blood from the lungs and pumps it to the left ventricle from where it is pumped back to the body. Both the filling and ejection processes are controlled by electrophysiological processes. At the cellular level the main components in the heart are cardiomyocytes, cardiac fibroblasts, endothelial cells and vascular smooth muscle cells [1]. Cardiomyocytes are subdivided into two types, namely the pacemaker-conduction and the contractile cardiomyocytes. Each cardiac cycle is initiated by sinoatrial cells located in the upper wall of the right atrium. Sinoatrial cells are pacemaker cardiomyocytes that can generate spontaneous action potentials, i.e. a rapid change in the membrane potential. Over a conduction system the action potential propagates throughout the whole heart so that the contractile cardiomyocytes in the atria and ventricles are electrically excited. Cardiomyocytes are composed of myofilaments enabling the cells to contract. Even pacemaker-conduction cardiomyocytes are able to contract but by far not as strong as the contractile cardiomyocytes. In a process called excitation-contraction coupling the action potential results in a release of Ca^{2+} from intracellular stores which activate the sarcomeres so that tension can be created and the cells can contract.

Computational cardiac models have been developed with the motivation to investigate the physiology and pathologies of the heart and ultimately to optimize therapies. In 1952, Hodgkin and Huxley published the first electrophysiological model of an excitable cell [2]. For a squid giant axon they linked the kinetics of ion channel conformation change with ion currents through the cell membrane and the change of the membrane potential. Ten years later, this groundbreaking work was extended by Noble to model the electrophysiology of cardiac myocytes [3]. Since then, the understanding of cellular mechanisms and the experimental potential has increased. This has led to the development and improvement of models for different human cardiomyocytes [4-7]. Since the models are already at a mature stage, they can serve as a basis to investigate the effect of various drugs on the cardiac electrophysiology [7, 8]. When these models are applied to tissues the action potential propagation from one cell to its neighboring cells needs to be taken into account. For this, the monodomain and bidomain reaction-diffusion equations are used. Bidomain equations account for the different electrical conductivities of the intracellular and extracellular spaces whereas only one conductivity is used in the monodomain equations. Differences between monodomain and bidomain results were reported to be extremely small [9] so that the monodomain equations with a much lower computational cost is widely preferred. Solving them with the Finite Element Method (FEM) gives the membrane averaged over a set of myocytes in each element.

While many questions can be addressed with electrophysiological models, others e.g. regarding the dilated cardiomyopathy necessitates a complete representation of the electromechanics. Improved computer performance has made it possible to develop FEM models where the electrophysiology is coupled with the mechanics. Electromechanical coupling is based on the relationship between the electrical activation of the tissue, the respective active tension generated by the sarcomeres and the resulting deformation [10]. Here, the electrophysiology is modeled on the cellular level [11-15] or is simplified using eikonal equations [16] or the Fitz-Hugh-Nagumo model [17,18]. There exist a wide range of electromechanical models from the cell [10,12] over the tissue [14] to the organ level including left ventricular models [11,15], models of both ventricles [12-15,17], and whole heart models [18]. They feature a varying degree of complexity with respect to the anatomical representation, associated mesh fineness, boundary conditions, material models, underlying electrophysiological models and coupling

models depending on the research objective. Different from the electrophysiological models electromechanical models are still in a maturing phase. Magnetic resonance imaging makes it now possible to create patient-specific highly resolved anatomical models [13], ventricle muscle fiber directions can be determined and assigned with a rule-based algorithm [19] and the orthotropic electric [20] and mechanical properties [21, 22] of the ventricular myocardium are well studied. However, there are still many tasks towards a highly sophisticated whole heart computer model. Examples include the model parametrization, verification, and validation procedures [23].

For thin cardiac tissue constructs these tasks have been addressed with a device called *CellDrum* [24, 25]**.** The *CellDrum* is a circular, 4 μm thin silicone membrane with a diameter of 16 mm. Human-induced pluripotent stem cell-derived cardiomyocytes (hiPSC-CM) are seeded and cultivated on top of the silicon membrane which is coated with fibronectin. The tissue monolayer has a thickness of up to 19 μm and consists of the following mixture: 60% myocardial ventricular, 35% atrial, and 5% nodal hiPSC-CM (Cor.4U, Axiogenesis AG, Germany). The cardiomyocytes live within a culture medium and beat autonomously as in the real heart. Clamped in a fixed ring the composite material can be inflated by a syringe pump and the resulting cellular contraction-dependent deflection is measured using a laser sensor. Thus, parameters for passive and coupling models can be determined [26]. Drugs have already been applied to the culture medium leading to phenomenologically observable changes in the beating frequency, deflection, contraction duration, activation time, relaxation time and resting time [25]. Frotscher et al. [14, 26, 27] developed an electromechanical model of the *CellDrum* which they parametrized, verified and validated using respective experiments. On the level of the electrophysiological cell models also the drug action was implemented. Until now, the effect of four drugs could be successfully simulated. Currently, the thin tissue construct is modeled as a materially and geometrically nonlinear shell whereas electrically it is viewed as a nonlinear three- dimensional continuum.

The next step is to perform experiments with thick cardiac tissue. For this, the mechanical model is modified towards a 3D continuum as well. Comparisons between the 2D shell formulation and 3D continuum formulation are presented. Furthermore, a new geometry is introduced to roughly predict the results of future experiments with thick cardiac tissue. Simulation results with and without the consideration of a chosen drug are shown.

2 ELECTROMECHANICAL MODEL

2.1 Electrophysiological model

Hodgkin-Huxley based cell models for sinoatrial [5], atrial [6] and ventricular [4] cardiomyocytes were employed, each having the general form

$$\frac{\partial V_m}{\partial t} = \frac{1}{C_m} I_{tot} \tag{1}$$

$$I_{tot} = I_{stim} - \sum_{i=1}^{n} I_i(g_j) \quad (j = 1, \dots, m) \tag{2}$$

$$\frac{\partial g_j}{\partial t} = \alpha_j^+(V_m)\left(1 - g_j\right) + \alpha_j^-(V_m) g_j, \tag{3}$$

where V_m is the cell membrane potential, C_m is the electrical capacitance of the cell membrane, I_{tot} is the total current for each cell model, I_{stim} is an electrical stimulus which is zero in the sinoatrial model, I_i are ionic currents related to the ion i and n is the number of ionic currents in the respective cell model. Gate variables g_j, usually one or two, control the opening and closure of each ion channels. Here, α_j^+ and α_j^- are experimentally determined opening and closure rates which depend on a threshold value of the membrane potential for each ion channel. Channel currents take the form

$$I_i = G_i \prod_{j=1}^{m} g_j (V_m - E_i), \tag{4}$$

where G_i is the maximum conductance of channel i and E_i is the reversal potential for the type of ion which flows through this channel.
Furthermore, the employed cell models provide ordinary differential equations for free intracellular sodium, potassium and calcium concentrations as well as for internal calcium stores.

Cellular interaction on the micro-scale level was took into account with a simple homogenization approach. Once the total current density of the sinoatrial model falls below a threshold $I_{tot} < -0.5\ \mu A \mu F^{-1}$, the atrial and ventricular model receive a stimulus

$$I_{stim} = -\frac{50 \mu A m m^{-3}}{C_m} \cdot \frac{V_{cell}}{A_m} \tag{5}$$

for 2 ms depending further on their ratio of cell volume V_{cell} to cell surface area A_m.
Concerning the respective volume fraction and cell volume to cell surface ratio of every cell model (s: sinoatrial, a: atrial, v: ventricular) the highly nonlinear source current per unit length reads

$$I_{src} = \left(\theta_s \frac{A_m^s}{V_{cell}^s} I_{tot}^s + \theta_a \frac{A_m^a}{V_{cell}^a} I_{tot}^a + \theta_v \frac{A_m^v}{V_{cell}^v} I_{tot}^v \right) (1 - \theta_{ECM}). \tag{6}$$

Here, also the volume fraction of the extracellular matrix θ_{ECM} including fibroblasts are taken into account. With this approach the microscopic cellular action potential are homogenized in order to get a macroscopic action potential that propagate throughout the tissue. The monodomain describing the action potential propagation reads

$$C \frac{\partial V}{\partial t} = \nabla(\mathbf{G}(\mathbf{B}) \nabla V) + I_{src}, \tag{7}$$

with the action potential V, capacitance C, isotropic conductance $\boldsymbol{G}$ and the left Cauchy-Green tensor $\mathbf{B}$.

2.2 Electromechanical coupling

Electromechanical coupling is described by the following two ordinary differential equations for each cell model:

$$\frac{\partial Ca_b}{\partial t} = f_1(Ca_i, Ca_b, T_0) \tag{8}$$

$$\frac{\partial z}{\partial t} = f_2(z, Ca_b, \mathbf{B}). \tag{9}$$

The calcium concentration Ca_b that is bound to troponin C in the myofilaments depends on the freely available calcium concentration Ca_i and on the cellular stress T_0. The strain-dependent state of activation is expressed by the activation variable $z \in (0,1)$. Finally, the cellular stress for each cell model is computed according to Niederer and Smith [10] by

$$T_0 = T_{ref}\big(1 + \beta_0(\lambda - 1)\big)K\frac{z}{z_{max}}, \tag{10}$$

with T_{ref} being the cellular reference stress, β_0 is a scalar determining the length dependence of the tension, λ is the one-dimensional cellular stretch in fiber direction, K reflects the binding velocity and z_{max} is the maximally available activation level. Due to a missing cell type specific parametrization an equal parametrization was used for all cell types. For the whole tissue construct the cellular reference stress was determined to be $T_{ref} = 0.5808$ kPa [26] which replaced the original model parameter [10].

2.3 Drug action

Drug action can be implemented in (4) using the conductance-block formulation where the maximal conductance of the channel i is reduced by the factor

$$g_i = g_{i,control}\left[1 + \left(\frac{D}{IC_{50\,j}}\right)^n\right]^{-1}. \tag{11}$$

Here, $g_{i,control}$ is the drug-free maximal conductance, D is the drug concentration the IC_{50} value represents the half-inhibitory value, i.e. the concentration of a given drug that will cause the current flowing through the channel i to be reduced by 50%. It has been shown that drug effects at steady-state concentration can be well represented by this model [28]. In this study, Verapamil is used as an example associated with blocking effects on the hERG-, L-type calcium- and sodium-channels of the ventricular cardiomyocytes. Respective IC_{50} values and effective free therapeutic plasma concentrations (EFTPC) used for D can be found in [8].

2.4 Mechanical model

Derivation of the mechanical properties of cardiac muscle tissue can be performed by employing either the active strain or active stress approach. The active strain approach utilizes a multiplicative split of the deformation gradient into passive $\mathbf{F}_\mathrm{p}$ and active deformation $\mathbf{F}_a$

$$\mathbf{F} = \mathbf{F}_p\mathbf{F}_a, \tag{12}$$

whereas in the active stress approach the total stress in the tissue is additively decomposed into the passive and active stress. Both approaches are considered to lead to comparable solutions [29].

Since the experimental parametrization was based on the level of stresses, the latter approach was used. Based on the work of Hunter et al. [30] the total Cauchy stress reads

$$\boldsymbol{\sigma} = \boldsymbol{\sigma}_p + \boldsymbol{\sigma}_a = 2J^{-1}\mathbf{B}\frac{\partial\psi}{\partial\mathbf{B}} - p\mathbf{I} + T(t,\mathbf{B})\mathbf{a}\otimes\mathbf{a}, \tag{13}$$

with the strain energy function ψ, the determinant of the deformation gradient J, the hydrostatic pressure p, the identity tensor $\mathbf{I}$, the active stress T being a scalar, the time t and the vector $\mathbf{a}$ oriented in the direction of the cardiac muscle fiber. Global isotropy of the muscle fibers is given in the thin cardiac tissue construct on the *CellDrum* [26], thus

$$\mathbf{a}\otimes\mathbf{a} = \mathbf{I}. \tag{14}$$

is assumed. Finally, the 2nd Piola-Kirchhoff stress $\mathbf{S}$ is given as

$$\mathbf{S} = \mathbf{S}_p + \mathbf{S}_a = 2\frac{\partial\psi}{\partial\mathbf{C}} - p\mathbf{C}^{-1} + T(t,\mathbf{C})\mathbf{C}^{-1}, \tag{15}$$

in terms of the right Cauchy-Green tensor $\mathbf{C}$. According to the experimentally measured pressure-deflection curves the quasi-incompressible hyperelastic neo-Hookean constitutive law

$$\psi = C_{10}(I_1 - 3) \tag{16}$$

was used where I_1 is the first invariant and $C_{10} = 0.0838284$ [26].

2.5 Finite Element Models

Finite element models were created for 19 µm and 100 µm thick cardiac tissue constructs. Due to symmetry only one quarter of the *CellDrum* was modeled. For a 19 µm thick cardiac tissue construct two models were developed. The first model is composed of a 2D mechanical model and a 3D electrical model. Shell formulation was used for the mechanical model which consists of 120 seven-node triangular elements. The electrical model consists of 7664 ten-node quadratic tetrahedral elements. The second model is completely formulated in 3D and both the mechanical and the electrical part are computed using the same mesh which is described above.

For a 100 µm thick cardiac tissue construct another 3D model was created. Here, the mesh consists of 7639 ten-node quadratic tetrahedral elements.

Firstly, the inflation process is simulated by applying a certain pressure to the clamped mechanical mesh. X Pa is necessary to displace the central point of the 2D 19 µm model to 1.2 mm. This has been experimentally validated [14]. Displacements are then projected onto the 3D electrical mesh. Subsequently, the autonomous cell contractions is simulated using an algorithm to solve the electromechanical problem which is described in [14]. When using the same mesh for the mechanical and the electrical part, the displacements do no longer need to be projected. The open source code *Code_Aster* was used to solve the nonlinear mechanical and electrical problem, whereas the cellular ordinary differential equations were solved internally using a fourth-order singly-diagonally implicit Runge-Kutta method.

3 RESULTS

3.1 Comparison between 2D and 3D mechanical model

Figure 1 shows the central node deflection of two 19 µm thick cardiac tissue construct models as a function of time. Models composed of a 2D and a 3D mechanics model are compared. As it was to be expected, the difference between both models is negligibly small. The same is true when the drug Verapamil is applied to the respective ventricular cell models [4]. Simulations with a low (25 nM) and a high effective free therapeutic plasma concentration (81 nM) were carried out. The resulting membrane potentials of the respective ventricular cell models correspond to [8]: the duration of the action potential decreases with increasing drug concentration. As distinguished from pure electrophysiology models *CellDrum* models are capable of predicting the drug effect on the deflection. Effects on the deflection are shown in Figure 2 for the second model: the deflection decreases with increasing drug concentration.

Figure 1: Central node deflection of a 19 µm thick cardiac tissue constructs. A 2D- (solid line) and a 3D-mechanical model (dashed line) are compared.

Figure 2: Effect of Verapamil on the central node deflection of a 19 µm thick cardiac tissue construct. The second 3D model was used. Results of the control (0 nM, solid line), low EFTPC (25 nM, dashed line), and high EFTPC (81 nM, dotted line) are shown.

3.2 Comparison between a 19 µm and a 100 µm thick cardiac tissue construct model

Figure 4 shows the time function of the central node deflection of two 3D cardiac tissue construct models. Models with different tissue construct thicknesses, 19 µm and 100 µm, are compared. In order to have the same start position, x Pa more pressure is needed to inflate the 100 µm model up to the same height as the 19 µm model. The deflection of the 100 µm model is lower compared to the 19 µm model. Furthermore, the effect of Verapamil on the deflection was investigated in both models. The application of 81 nM Verapamil results in a peak deflection difference of x1 (x2) mm in the 19 (100) µm models.

Figure 3: Central node deflection of two differently thick tissue constructs. 19 µm thick (solid line) and 100 µm thick (dashed line) cardiac tissue construct models are compared. Comparisons were made with no addition of a drug.

4 OUTLOOK

In the present model the electric and passive material properties were modeled to be isotropic according to global isotropy of the cardiac tissue on the *CellDrum*. However, myocardial tissue of the left ventricle is orthotropic in both electrical [20] and passive mechanical properties [21] and thus, it is unsuitable for heart models. Currently, an orthotropic model is developed which is described in the following.

Myocardial tissue is organized in layers with collagen fibers between the sheets and are referred to a right-handed orthonormal coordinate system with the fiber axis $\mathbf{f}_0$, the sheet axis $\mathbf{s}_0$, and sheet normal axis $\mathbf{n}_0$ (Figure 4).

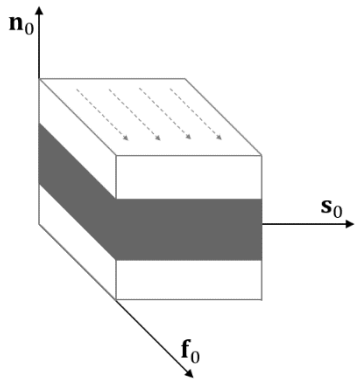

Figure 4: Right-handed orthonormal coordinate system with fiber axis $\mathbf{f}_0$, sheet axis $\mathbf{s}_0$ and sheet-normal axis $\mathbf{n}_0$ in the layered organization of myocardial tissue. The fiber direction is indicated with dashed arrows.

Orthotropic electrical behavior is considered in the monodomain equation (7). Here, an anisotropic conductance tensor $\mathbf{G}$ is used in order to incorporate differences in the action potential propagation in all axes as has been done in [13]. Orthotropic passive material behavior is implemented using the strain energy function published Holzapfel and Ogden [21]

$$\psi = \frac{a}{2b}\exp[b(I_1 - 3)] + \sum_{i=f,s} \frac{a_i}{2b_i}\{exp[b_i(I_{4i} - 1)^2] - 1\} + \frac{a_{fs}}{2b_{fs}}\left[exp\left(b_{fs}I_{8fs}^2\right) - 1\right], \quad (17)$$

where a, b, a_f, a_s, b_f, b_s, a_{fs} and b_{fs} are eight positive material constants which can be derived from [22]. The given strain energy function consists of an isotropic term in I_1, a transversely isotropic term in I_{4f} and I_{4s} and an orthotropic term in I_{8fs}. The respective invariants read

$$I_1 = tr\mathbf{C}, \quad I_{4f} = \mathbf{f}_0 \cdot (\mathbf{C}\mathbf{f}_0), \quad I_{4s} = \mathbf{s}_0 \cdot (\mathbf{C}\mathbf{s}_0), \quad I_{8fs} = \mathbf{f}_0 \cdot (\mathbf{C}\mathbf{s}_0). \quad (18)$$

Using the *CellDrum* geometry the fiber direction will be set to be orientated radially from the center to the edge. Analogue experiments might be possible in the future using mainly myocardial ventricular cells which are cultivated in a way that they grow in the desired direction. This allows to parameterize the active stress model (10) by measuring the cell type specific reference stress having the mentioned passive stress model as basis. All in all, improved models can help to better investigate the effect of drugs *in-silico*.

REFERENCES

[1] A.R. Pinto, A. Ilinykh, M.J. Ivey, J.T. Kuwabara, M.L. D´Antoni, R. Debuque, A. Chandran, L. Wang, K. Arora, N.A. Rosenthal, M.D. Tallquist, Revisiting cardiac cellular composition. *Circulation Research*, **118**, 400-409, 2016.

[2] A.L. Hodgkin, A.F. Huxley, A quantitative description of membrane current and its application to conduction and excitation in nerve. *Journal of Physiology*, **117**, 500-544, 1952.

[3] D. Noble, A modification of the Hodgkin-Huxley equations applicable to Purkinje fibre action and pace-maker potentials. *Journal of Physiology*, **160**, 317-352, 1962.

[4] K.H.W.J. ten Tusscher, A.V. Panfilov, Alternans and spiral breakup in a human ventricular tissue model. *American Journal of Physiology – Heart and Circulatory Physiology*, **29**, H1088-H1100, 2006.

[5] N.J. Chandler, I.D. Greener, J.O. Tellez, S. Inada, H. Musa, P. Molenaar, D. DiFrancesco, M. Baruscotti, R. Longhi, R.H. Anderson, R. Billeter, V. Sharma, D.C. Sigg, M.R. Boyett, H. Dobrzynski, Molecular architecture of the human sinus node: insights into the function of the cardiac pacemaker. *Circulation*, **119**, 1562-1575, 2009.

[6] M. Paci, J. Hyttinen, K. Aalto-Setälä, S. Severi, Computational models of ventricular- and atrial-like human induced pluripotent stem cell derived cardiomyocytes. *Annals of Biomedical Engineering*, **41**, 2334-2348, 2013.

[7] O.V. Aslanidi, M. Al-Owais, A.P. Benson, M. Colman, C.J. Garratt, J.P. Greenwood, A.V. Holden, S. Kharche, E. Kinnell, E. Pervolaraki, S. Plein, J. Stott, H. Zhang, Virtual tissue engineering of the human atrium: modeling pharmacological actions on atrial arrhythmogenesis. *European Journal of Pharmaceutical Sciences*, **46**, 209-221, 2012.

[8] G.R. Mirams, Y. Cui, A. Sher, M. Fink, J. Cooper, B.M. Heath, N.C. McMahon, D.J. Gavaghan, D. Noble, Simulation of multiple ion channel block provides improved early prediction of compounds´ clinical torsadogenic risk. *Cardiovascular Research*, **91**, 53-61, 2011.

[9] M. Potse, B. Dubé, J. Richer, A. Vinet, R.M. Gulrajani, A comparison of monodomain and bidomain reaction-diffusion models for action potential propagation in the human heart, *IEEE Transactions on Biomedical Engineering*, **53**, 2425-2435, 2006.

[10] S.A. Niederer, N.P. Smith, An improved numerical method for strong coupling of excitation and contraction models in the heart, *Progress in Biophysics and Molecular Biology*, **96**, 90-111, 2008.

[11] T.S.E. Eriksson, A.J. Prassl, G. Plank, G.A. Holzapfel, Modeling the dispersion in electromechanically coupled myocardium. *International Journal of Numerical Methods in Biomedical Engineering*, **29**, 1267-1284, 2013.

[12] R. Ruiz-Baier, A. Gizzi, S. Rossi, C. Cherubini, A. Laadhari, S. Filippi, A. Quarteroni, Mathematical modelling of active contraction in isolated cardiac myocytes, *Mathematical Medicine and Biology*, **31**, 259-283, 2014.

[13] C.M. Augustin, A. Neic, M. Liebmann, A.J. Prassl, S.A. Niederer, G. Haase, G. Plank, Anatomically accurate high resolution modeling of human whole heart electromechanics: a strongly scalable algebraic multigrid solver method for nonlinear deformation, *Journal of Computational Physics*, **305**, 622-646, 2016.

[14] R. Frotscher, D. Muanghong, G. Dursun, M. Goßmann, A. Temiz-Artmann, M. Staat, Sample-specific adaption of an improved electromechanical model of in vitro cardiac tissue, *Journal of Biomechanics*, 2016 (in press).

[15] A. Quarteroni, T. Lassila, S. Rossi, R. Ruiz-Baier, Integrated heart – Coupling multiscale and Multiphysics models for the simulation of the cardiac function, *Computer Methods in Applied Mechanics and Engineering*, 2016 (submitted), https://www.mate.polimi.it/biblioteca/add/qmox/05-2016.pdf.

[16] M. Sermesant, R. Chabiniok, P. Chinchapatnam, T. Mansi, F. Billet, P. Moireau, J.M. Peyrat, K. Wong, J. Relan, K. Rhode, M. Ginks, P. Lambiase, H. Delingette, M. Sorine, C.A. Rinaldi, D. Chapelle, R. Razavi, N. Ayache. Patient-specific electromechanical models of the heart for the prediction of pacing acute effects in CRT: a preliminary clinical validation. *Medical Image Analysis*, **16**, 201-215, 2012.

[17] E. Berberoglu, H.O. Solmaz, S. Göktepe, Computational modeling of coupled cardiac electromechanics incorporating cardiac dysfunctions. *European Journal of Mechanics – A/ Solids*, **48**, 60-73, 2014.

[18] B. Baillargeon, N. Rebelo, D.D. Fox, R.L. Taylor, E. Kuhl, The Living Heart Project: A robust and integrative simulator for human heart function. *European Journal of Mechanics –A/ Solids*, **48**, 38-47, 2014.

[19] J.D. Bayer, R.C. Blake, G. Plank, N.A. Trayanova, A novel rule-based algorithm for assigning myocardial fiber orientation to computational heart models, *Annals of Biomedical Engineering*, **40**, 2243-2254, 2012.

[20] B.J. Caldwell, M.L. Trew, G.B. Sands, D.A. Hooks, I.J. LeGrice, B.H. Smaill, Three distinct directions of intramural activation reveal nonuniform side-to-side electrical coupling of ventricular myocytes. *Circulation: Arrhytmia and Electrophysiology*, **2**, 433-44, 2009.

[21] G.A. Holzapfel, R.W. Ogden, Constitutive modeling of passive myocardium: a structurally based framework for material characterization. *Philosophical Transactions of the Royal Society A – Mathematical, Physical and Engineering Sciences*, **367**, 3445-3475, 2009.

[22] G. Sommer, A.J. Schriefl, M. Andrä, M. Sacherer, C. Viertler, H. Wolinski, G.A. Holzapfel, Biomechanical properties and microstructure of human ventricular myocardium, *Acta Biomaterialia*, **24**, 172-192, 2015.

[23] P. Pathmanathan, R.A. Gray, Ensuring reliability of safety-critical clinical applications of computational cardiac models. *Frontiers in Physiology*, **4**, 358, 2013.

[24] P. Linder, J. Trzewik, M. Rüffer, G. Artmann, I. Digel, R. Kurz, A. Rothermel, A. Robitzki, A. Temiz-Artmann, Contractile tension and beating rates of self-exciting monolayers and 3D-tissue constructs of neonatal rat cardiomyocytes, *Medical & Biological Engineering & Computing*, **48**, 59-65, 2010.

[25] M. Goßmann, R. Frotscher, P. Linder, S. Neumann, R. Bayer, M. Epple, M. Staat, A. Temiz-Artmann, G. Artmann, Mechano-pharmacological characterization of cardiomyocytes derived from human induced stem cells. *Cellular Physiology and Biology*, 2016 (in press)

[26] R. Frotscher, M. Goßmann, H.J. Raatschen, A. Temiz-Artmann, M. Staat, *Simulation of cardiac cell-seeded membranes using the edge-based smoothed FEM.* In: H. Altenbach,

G.I. Mikhasev (eds), *Shell and membrane theories in mechanics and biology: From macro- to nanoscale structures*, Springer, 2015.

[27] R. Frotscher, J.P. Koch, M. Staat, Computational investigation of drug action on human-induced stem cell derived cardiomyocytes. *Journal of Biomechanical Engineering*, **137**, 071002-071002-7, 2015.

[28] T. Brennan, M. Fink, B. Rodriguez, Multiscale modeling of drug-induced effects on cardiac electrophysiological activity. *European Journal of Pharmaceutical Sciences*, **36**, 62-77, 2009.

[29] A. Gizzi, C. Cherubini, S. Filippi, A. Pandolfi, Theoretical and numerical modeling of nonlinear electromechanics with applications to biological active media. *Communications in Computational Physics*, **17**, 93-126, 2015.

[30] P. J. Hunter, A.D. McCulloch, H.E.D.J. ter Keurs, Modelling the mechanical properties of cardiac muscle. *Progress in Biophysics and Molecular Biology*, **69**, 289–331, 1998.